

## OW\_09

# 應用時域模擬於固定式離岸風力機套管基礎之疲勞壽命分析 Fatigue Life Evaluation using Time-domain Simulation for Bottom-fixed Jacket Foundation of Offshore Wind Turbine

林宗岳<sup>1\*</sup>、范秉天<sup>1</sup>、吳凱洋<sup>1</sup>、黃心豪<sup>2</sup>、簡志宇<sup>2</sup>

<sup>1</sup>財團法人中國驗船中心

<sup>2</sup>國立台灣大學 工程科學及海洋工程學系暨研究所

Tsung-Yueh Lin<sup>1\*</sup>, Bryan Nelson<sup>1</sup>, Yann Quémener<sup>1</sup>, Hsin-Haou Huang<sup>2</sup>, Chi-Yu Chien<sup>2</sup>

<sup>1</sup> Research Department, CR Classification Society, Taiwan

<sup>2</sup> Department of Engineering Science and Ocean Engineering, National Taiwan University, Taiwan

\* tylin@crlclass.org

### 摘要

本研究目標為以時域法分析套管式離岸風力機基礎結構的疲勞壽命。此風力機容量為 3.6 MW，設定場址位於福海離岸風場。海上環境量測及統計資料來源取自三年期的初期場址調查，得到風況及海況的機率散佈表和聯合機率表。海況以有義波高和零上切週期轉換成波浪頻譜模型，再由 HydroCRest 計算圓管構件之波浪負荷。風負荷分析方法使用 BEM 準穩態時域分析法，紊流模型採用 IEC 標準。本研究藉由有限元素分析結果推導接點公稱應力的閉合形式解，以縮短有限元素分析時間近千倍。熱點應力以接點公稱應力乘以應力集中係數計算。最後套用雨流計數法和查詢 S-N 曲線，得到接點疲勞壽命。結果顯示，數十日的模擬時間即能得到穩定且收斂的 20 年疲勞累積破壞值。

關鍵詞：離岸風力機，套管式基礎，疲勞分析，雨流計數法。

### Abstract

This study evaluated the fatigue life of the jacket support structure of a 3.6 MW wind turbine operating in Fuhai Offshore Wind Farm by time-domain simulations. The long term statistical environment was based on a preliminary site survey that adequately served as the basis for a convergence study for an accurate fatigue life evaluation. The wave loads were determined by the Morison equation, executed via the in-house HydroCRest code, and the wind loads on the wind turbine rotor were calculated by an unsteady BEM method. The Finite Element model of the wind turbine was built using Beam elements. However, to reduce the time of computation, the hot spot stress evaluation approach combined FE-derived Closed-Form expressions of the nominal stress at the tubular joints and stress concentration factors. Finally, the fatigue damage was assessed using the Rainflow Cycle Counting scheme and adequate SN curves. The results showed that after a dozen days of simulated life time, the accumulated fatigue damage prediction converged to a stable 20-year fatigue damage.

*Keywords: Offshore wind turbine, Jacket foundation, Fatigue analysis, Rainflow counting method.*

### I. Introduction

Taiwan has recently started to evaluate the potential for offshore wind energy production off its west coast, which was selected by 4C Offshore Limited as one of the world's best wind locations [1], having considerable development potential due to high wind energy, stable wind speed, and shallow water depth.

Previously, the authors [1, 2] showed that typhoon conditions are crucial design problems for the ultimate strength of the unit. However, fatigue strength can be just as significant, especially at the tubular joint connections of the jacket support structure that are subjected to numerous load cycles during the 20 years of design life. Therefore, this study conducted time-domain simulations to reproduce accurately the long-term evolution of the wind and wave loads on the unit and to evaluate the corresponding structural response. However, time-domain simulations can be very time consuming. This study thus proposed load generation models and structural response approaches that are a good trade-off between time-efficiency and simulation accuracy. The calculations were conducted according to DNV-GL Guideline [3], in compliance with the IEC's 61400-1 International Standard [4].

The long-term environmental conditions are described in the second section of this paper, and the short-term conditions, based on IEC and DNV guidelines, and the numerical models employed to calculate the wind and hydrodynamic loads are described in the third part. The fourth part of the present paper presents the hot spot stress evaluation approach that combined FE-derived Closed-Form expressions of the nominal stresses at the tubular joints and stress concentration factors. Finally, the fatigue damage was assessed using the Rainflow Cycle Counting scheme. The fatigue life assessment results and suggestions for future improvements are discussed in the Conclusions.

### II. Long-term environmental statistics

The long-term statistical environment was based on a preliminary site survey gathered over three years. Scatter diagrams and joint probability tables were collated to produce a covariance matrix of the five considered environmental load parameters, namely wave height, period,

and direction, and wind speed and direction. This allowed for the stochastic generation of 20 years of weather states, which served as the basis for statistically accurate wind and wave load calculations with which to implement fatigue life evaluations.

### III. Short-term environmental loads

For each sea state, the selected JONSWAP sea spectrum [12] and directional spreading function were applied to obtain an irregular, time-varying flow field, for which the consequent wave loads were determined by the Morison equation, as expressed in Eq. (1), by executed via the in-house HydroCRest code. The determination of coefficients follows DNV-GL Guideline [3], where the slamming term  $F_s$  is neglected in normal wave conditions.

Based on the superposition solution of potential flow theory, an irregular sea surface can be decomposed into infinite numbers of regular component waves, which are formulated by amplitude, direction, frequency, and phase, shown in Figure 1 [13]. For a given power spectrum, i.e. directional JONSWAP, Eq. (2), the amplitude is calculated by Eq. (3). The JONSWAP formula is expressed by Eq. (4), and the directional spreading function is the cosine-power equation, as Eq. (5). Two demonstrated spectrums at  $H_s = 1.4\text{m}$  and  $4.0\text{m}$  with different main directions are shown in polar plot in Figure 2. A GPU accelerator was utilized [14] to speed up the wave load simulation for parallel processing thousands of component waves and element nodes and then sum reduction of each line load to an overall overturning moment to comply with the close-form formulation of FEA. Figure 3 shows the nodal forces and total force in HydroCRest. Figures 4, 5 plot the time series of OTM magnitude and directional distribution of the two sea states.

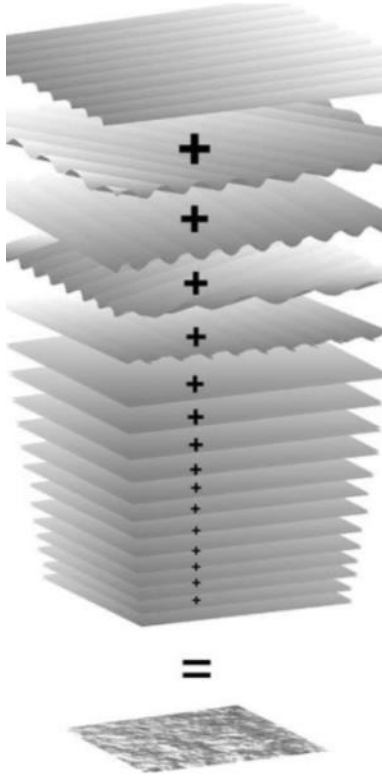


Figure 1. Superposition of regular waves for an irregular sea

$$F_M = \rho_{sw} \cdot C_M \cdot A \cdot \dot{v} + \frac{1}{2} \rho_{sw} \cdot C_D \cdot D \cdot v \cdot |v| + F_s \quad (1)$$

$$E(\omega, \theta) = S_J(\omega) D(\omega, \theta) \quad (2)$$

$$a(\omega_n, \theta_n) = \sqrt{2 \int_{\Delta\omega_n} \int_{\Delta\theta_n} E(\omega, \theta) d\theta d\omega} \\ \approx \sqrt{2 S_J(\omega_n) D(\omega_n, \theta_n) \Delta\theta \Delta\omega} \quad (3)$$

$$S_J(\omega) = \frac{\alpha g^2}{\omega^5} \exp\left(-1.25 \left(\frac{\omega_p}{\omega}\right)^4\right) \gamma^{\exp\left(-\frac{(\omega-\omega_p)^2}{2\sigma^2\omega_p^2}\right)}$$

, where

$$\alpha = \frac{4\pi^3 H_s^2}{g^2 T_z^4} \\ \gamma = 7.0 \cdot \left(1.0 - \frac{0.218 \cdot 10^{-4} \cdot g^2 T_z}{H_s^2}\right) \quad (4)$$

$$\omega_p = \frac{2\pi}{T_z} \sqrt{\frac{5.0 + \gamma}{10.89 + \gamma}}$$

$$\sigma = \begin{cases} 0.07 & , \text{if } \omega \leq \omega_p \\ 0.09 & , \text{if } \omega > \omega_p \end{cases}$$

$$D(\omega, \theta) = N(s(\omega)) \cos^{2s(\omega)}\left(\frac{\theta_w - \theta}{2}\right)$$

, where

$$N(s(\omega)) = \frac{1}{2\sqrt{\pi}} \frac{\Gamma(s(\omega) + 1)}{\Gamma(s(\omega) + 1/2)} \quad (5)$$

$$s(\omega) = 17.013 \left(\frac{\omega}{\omega_p}\right)^\mu$$

$$\mu = \begin{cases} 5 & , \text{if } \omega \leq \omega_p \\ -2.5 & , \text{if } \omega > \omega_p \end{cases}$$

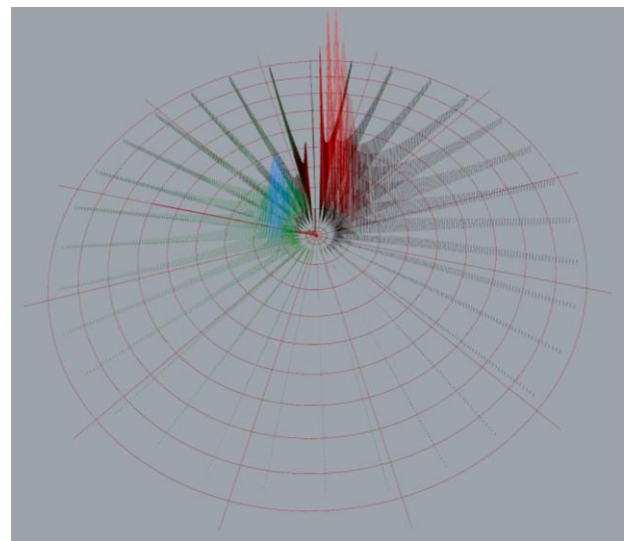


Figure 2. Sampling of component waves in two directional JONSWAP spectrums

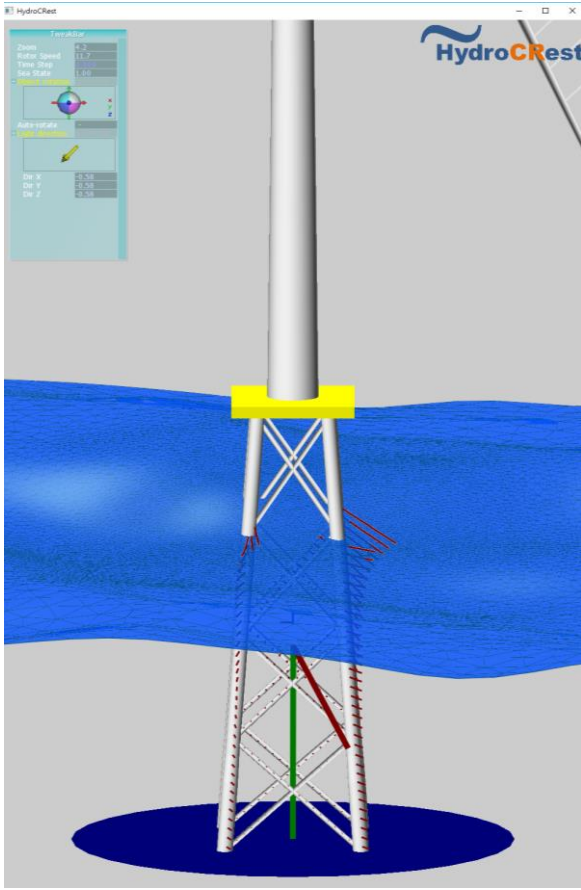


Figure 3. Nodal load distribution on members (thin lines) and total load on center of force (thick lines) in irregular sea

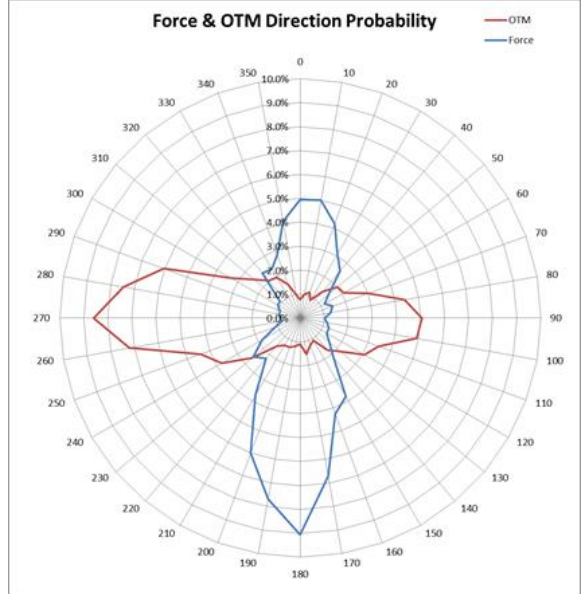


Figure 4. Directional distribution of total force and moment

On the wind load, the concept of wind turbulence is explained in DNV [3] as “the natural variability of the wind speed about the mean wind speed  $U_{10}$  in a 10-minute period” for which “the short-term probability distribution for the instantaneous wind speed  $U$  can be assumed to be a normal distribution” with standard deviation  $\sigma_U$ . Furthermore, “for a given value of  $U_{10}$ , the standard deviation  $\sigma_U$  of the wind speed exhibits a natural variability from one 10-minute period to another.”

In the present study, the stochastically generated short term wind states were modeled on the IEC 61400-1 [4] Normal Turbulence Model (NTM), with a reference turbulence intensity of  $I_{ref} = 0.16$ , as per the requirement of the Taiwanese Ministry of Economic Affairs [5] that the pilot wind turbine to be installed in the Fuhai offshore wind farm must be IEC 61400-1 Class I<sub>A</sub> compliant. Following the NTM, the mean value  $\bar{\sigma}$  and the standard deviation of the standard deviation of the wind speed  $\sigma_U$  for a given  $U_{10}$  are calculated by Eqs. (6, 7), respectively:

$$\bar{\sigma} = I_{ref} (0.75 \cdot U_{10} + 3.8) \quad (6)$$

$$\sigma_{\sigma} = 1.4 \cdot I_{ref} \quad (7)$$

However, an inherent problem with using random number generators to produce wind states is that short-term wind speed values are not statistically independent [4, 6]. Thus, in order to generate a more realistic short-term wind state, the wind speed fluctuations were calibrated against real on-site data [7] by taking the fast Fourier transforms (FFT) of the wind speed data over consecutive 10-minute periods, and then reconstructing the signals over different frequency ranges. It was observed that summing the harmonics of periods  $T \geq 30$  s captured most of the major fluctuations, while summing the harmonics of periods  $T \geq 5$  s almost perfectly matched the original data (Fig. 6). It was therefore decided to generate a discrete-time random signal with a normal distribution and a time step of 30 s, and to then add Gaussian noise at 5 s intervals, where the mean and standard deviation input parameters are designed so as to produce a final signal which conforms to the IEC NTM. The results of one of these stochastically generated short-term wind states is shown in Figure 7.

Due to the large number of wind load calculations to be made over the simulated life time, an unsteady blade element momentum method (UBEM) was adopted to calculate the aerodynamic loads on the wind turbine. Due to its maturity, the BEM is widely employed for the design and analysis of wind turbines [10]. The blade element theory discretises the rotor into a number of 2D airfoil sections, such that the axial and tangential loads on each 2D section may be calculated from the respective airfoil’s lift and drag characteristics for the respective local relative flow velocity and angle. These local loads are then integrated along the length of the rotor blades and multiplied by the number of blades, as per Eq. (8), to determine the total thrust and rotor torque:

$$dF_N = n_B \frac{1}{2} \rho U_{rel}^2 \int_0^R (C_l \cos \varphi + C_d \sin \varphi) c dr \quad (8)$$

$$dQ = n_B \frac{1}{2} \rho U_{rel}^2 \int_0^R (C_l \sin \varphi + C_d \cos \varphi) c r dr$$

The effects of the wind turbine tower on the upstream flowfield were modelled by assuming potential flow around a circular cylinder [7], such that the radial and angular components of the flow velocity at a considered point are given by Eq. (9):

$$U_r = U_\infty \left( 1 - \frac{R^2}{r^2} \right) \cos \theta \quad (9)$$

$$U_\theta = -U_\infty \left( 1 + \frac{R^2}{r^2} \right) \sin \theta$$

A wind shear profile was included, such that the wind velocity at height  $z$  for a specified hub height velocity  $U(H)$  is given by Eq. (10):

$$U(z) = U(H) \cdot \left( \frac{z}{H} \right)^\alpha \quad (10)$$

where the power law exponent for offshore locations is taken as  $\alpha = 0.14$ , in accordance with DNV [8].

The UBEM was validated against the power curve provided by the 3.6 MW wind turbine manufacturer [11], and was found to correlate very well with the official data (Fig. 8).

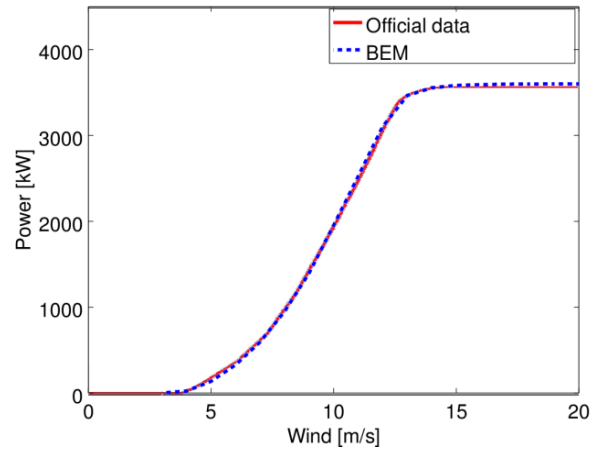


Figure 8. Compared wind power curves

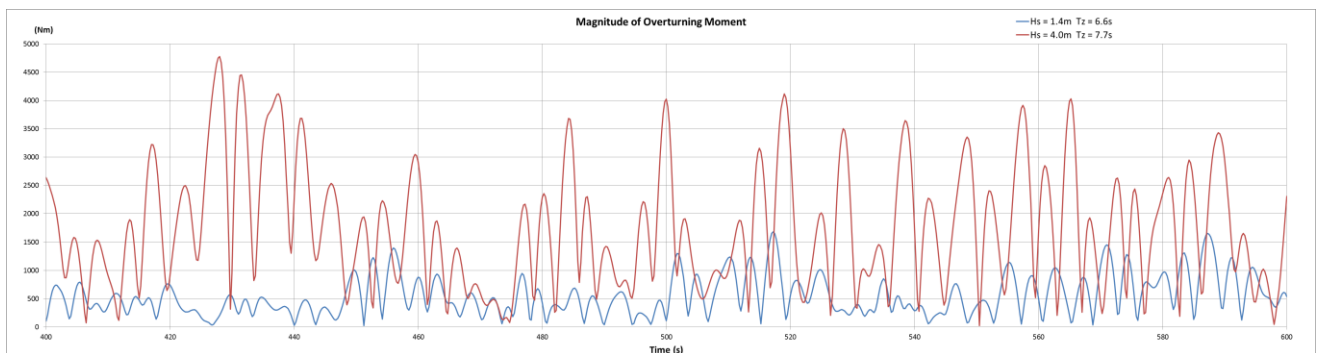


Figure 5. Time-history of magnitudes of overturning moment in two sea states

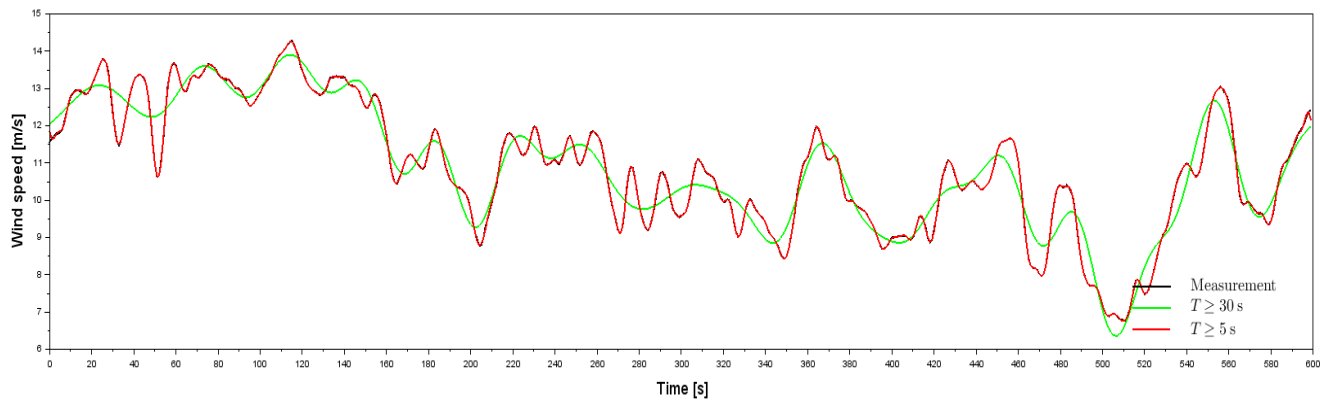


Figure 6. Reconstructed signals vs. measured data

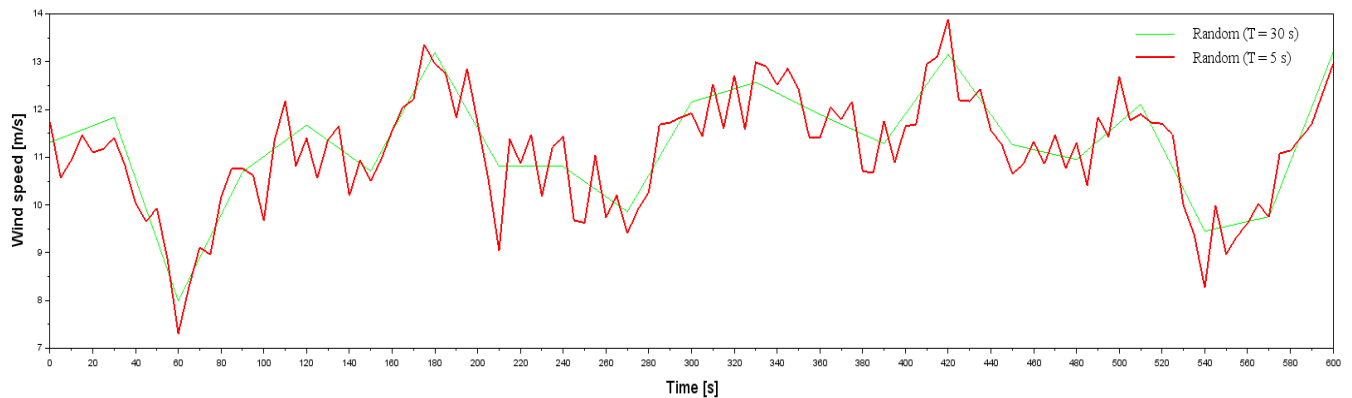


Figure 7. Stochastically generated short-term wind condition showing major/minor fluctuations

#### IV. Fatigue life assessment

Using beam elements, a structural finite element model of the unit was built, which included the tower, the mass of the rotor nacelle assembly, the jacket, and the four piles, for which the interaction with the soil was reproduced using nonlinear elastic spring connectors. The wind thrust at the nacelle and hydrodynamic line loads on the jacket were produced using HydroCRest. Figure 9 shows the finite element model of the offshore wind turbine. However, the time of computation required to conduct the static Finite Element Analyses was approximately of 0.5 s per time step, which would require several weeks of computations for the millions of wind and wave induced load cycles to simulate during a 20-year design life. A faster approach was thus adopted to conduct rapid fatigue life assessments that consisted in deriving from FEA results the Closed-Form (CF) expressions of the nominal stress at the tubular joints connection in the jacket structure as a function of four global load parameters (see Fig. 9):

- the amplitude and direction of the hydrodynamic load (i.e. wave and current on jacket) induced overturning moment at the mudline ( $OTM_{Hydro}$  and  $\beta_{Hydro}$ ), and
- the amplitude and direction of the wind load (i.e. tower and blades) induced overturning moment at the mudline ( $OTM_{Wind}$  and  $\beta_{Wind}$ ).

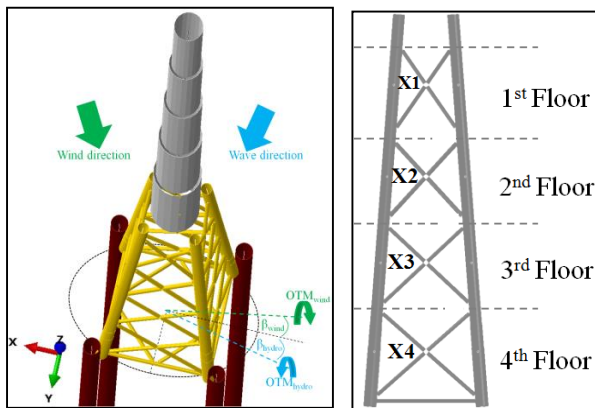


Figure 9. Offshore wind turbine finite element model and Closed-Form expressions load parameters at the mudline.

The structural stress assessment at the joints for more than 8000 wind and wave load combinations were conducted through static FEAs that corresponded to various combinations in amplitude and directions of the 4 global load parameters entailed in the closed-form expression. A unique regression expression was then fitted for each FE-nodal stress at the joints connection through a set of constant parameters ( $C_1$  to  $C_8$ ) as provided in Eq. (11). Finally, the hot spot stress at 8 spots around the circumference was obtained by including the stress concentration factors accordingly to DNV-GL RP-C203 [9].

$$\sigma_{nom} = (C_1 \cdot OTM_{Wind} + C_2) \cdot \cos(\beta_{Wind} + C_3) + C_4 \cdot \cos(\beta_{Hydro} + C_5) + (C_6 \cdot OTM_{Hydro}^2 + C_7 \cdot OTM_{Hydro} + C_8) \quad (11)$$

Figure 10 shows the nominal stresses at 504 nodes in the global FE model produced by the Closed-Form

expressions and those extracted from the global FEA for 8321 FE-load combinations and two different water depths. The Closed-Form expressions were determined using the FE-results corresponding to the average high-tide water depth FE-load cases, and in Fig.10 (upper), it can be observed that the Closed-Form predictions were very accurate. The same Closed-Form expressions were then employed to reproduce the nominal stresses computed by the low-tide FE-load cases, and in Fig.10 (lower), it appeared that the accuracy was still satisfactory, despite a hydrodynamic line load distribution obtained for a water depth 3.5 m smaller. In the future, the structural response of the global FE model of the offshore wind turbine will be conducted for the short-term condition that was found to contribute the most to the fatigue life, as predicted by the Closed-Form approach. The comparison of the fatigue damage results will make it possible to conclude on the accuracy of the Closed-Form nominal stress expressions approach, which enabled reducing significantly the time of computation to approximately 0.722 ms per time step.

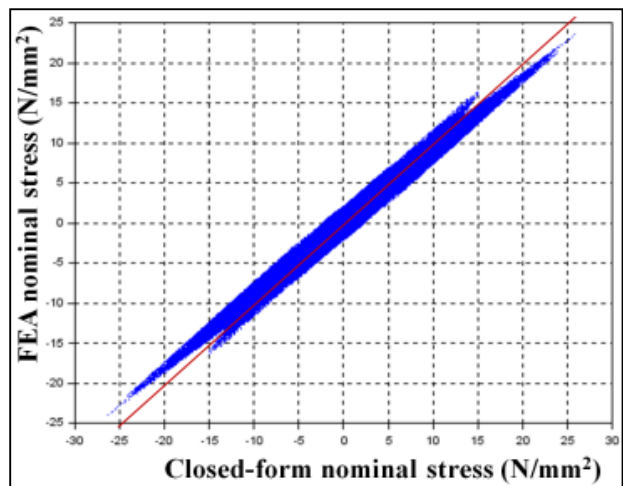
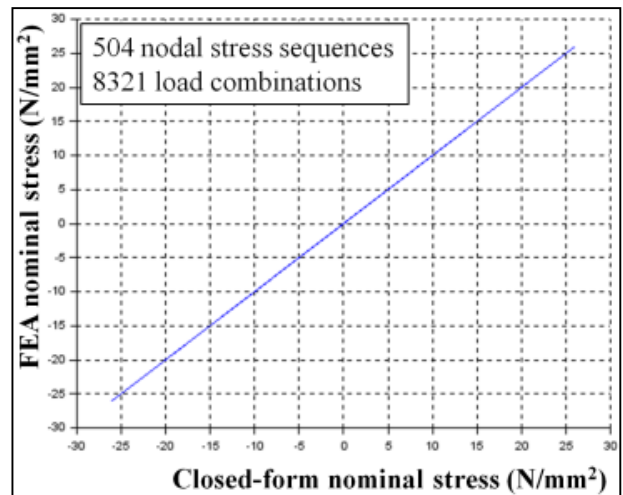


Figure 10. Nominal stress Closed-Form predictions vs. global FEA results for average high-tide (upper) and low-tide (lower) water depth FE-load cases.

Using the Closed-Form expressions, the 10-min short-term sequences of hot spot stress at the braces X-joints (see Fig. 9) of one face of the jacket were derived from the short-

term sequences of wind and wave loads previously generated. The hot spot stress range distribution was then extracted through a Rainflow Cycle Counting scheme and the fatigue damage was evaluated for the 'T' class S-N curve as recommended by DNV-GL [9] for tubular members. The fatigue damage (D) of each 10-min short-term condition was accumulated to the total fatigue damage for the 4000 simulated short-term conditions, which resulted in a total simulated life time of 28 days. Figure 11 presents the accumulated fatigue damage for the 4 X-joints. It can be observed that the X-joint No.4 (see Fig. 11) is the most critical with a fatigue damage of approximately  $1 \times 10^{-5}$  produced for 28 days of simulated life.

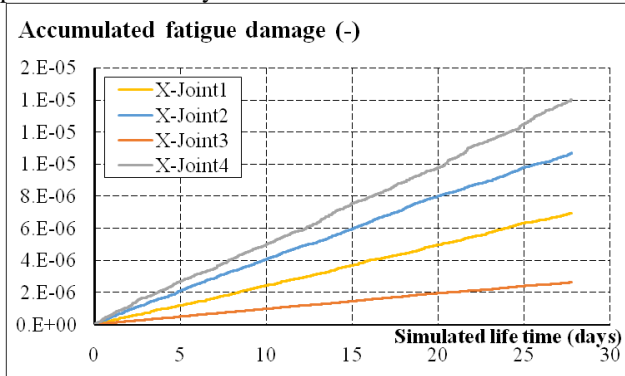


Figure 11. Accumulated fatigue damage for the 4 X-joints.

The fatigue damage evolution was then scaled up to the 20 years design life following the expression provided in Eq. (12).

$$D_{20yrs} = \frac{20}{t} D(t) \quad (12)$$

Figure 12 shows the accumulated fatigue damage scaled up to the 20 years design life. It appeared that the fatigue damage was much lower than 1.0, therefore the fatigue life of the investigated X-joints was found satisfactory. It can also be observed that the fatigue life tends to converge after 5 to 10 days of simulated life. However, the accuracy of the convergence cannot be confirmed after 28 days of simulated life. Longer simulation are thus required in order to determine an optimal life time of simulation that, in the future, could be employed to conduct time-efficient fatigue assessment entailing global finite element analyses.

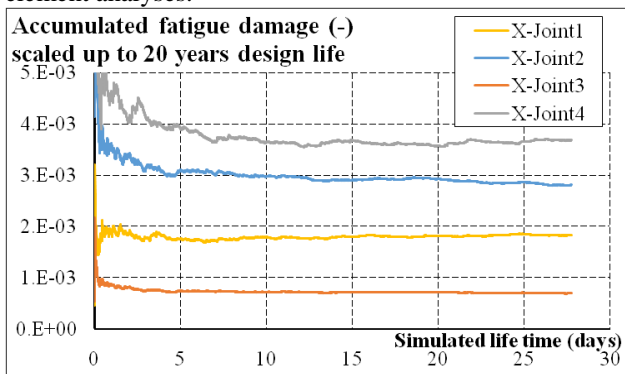


Figure 12. Accumulated fatigue damage for the 4 X-joints scaled up to 20 years design life.

## V. Conclusions

This study presented a fatigue life evaluation methodology for fixed-type offshore wind turbine foundations using time-domain simulations and the Rainflow Cycle Counting method. A long-term statistical environment, based on a preliminary site survey, and comprising 10-minute short term conditions based on IEC and DNV guidelines, was generated for a 28 day simulated life. The accumulated fatigue damage, after scaling up to 20 years, was observed to converge after 5 to 10 days of simulated life. However, the accuracy of the convergence cannot be confirmed after just 28 days of simulated life. Longer simulations are thus required in order to determine an optimal life time of simulation that, in the future, could be employed to conduct time-efficient fatigue assessment entailing global finite element analyses.

In the future, the structural response of the global FE model of the offshore wind turbine will be conducted for the short-term condition that was found to contribute the most to the fatigue life, as predicted by the Closed-Form approach.

## References

- [1] T.Y. Lin, Y. Quéméner, "Extreme Typhoon Loads Effect on the Structural Response of Offshore Meteorological Mast and Wind Turbine", Proceedings of the ASME 2016 35th International Conference on Ocean, Offshore and Arctic Engineering, OMAE2016, 19-24 Jun., 2016, Busan, Korea.
- [2] B. Nelson, T.Y. Lin, Y. Quéméner, H.H. Huang, C.Y. Chien, "Extreme Typhoon Loads Effect on the Structural Response of an Offshore Wind Turbine", Proceedings of 7th PAAMES and AMEC2016, 13-14 Oct., 2016, Hong Kong.
- [3] DNVGL (2014), Design of Offshore Wind Turbine Structures, DNVGL-OS-J101.
- [4] IEC, Wind turbines – Part 1: Design requirements, IEC International Standard 61400-1, 2005.
- [5] Ministry of Economic Affairs of Taiwan (R.O.C.), "風力發電離岸系統示範獎勵辦法 (Regulations for Demonstration and Rewards of Offshore Wind Power System)", Taiwan, 2012.
- [6] "Offshore Wind Farms Database," <http://www.4coffshore.com>, 2015
- [7] L. Kristensen, G. Jensen, A. Hansen, and P. Kirkegaard, "Field Calibration of Cup Anemometers", Risø-R-1218(EN), Risø National Laboratory, Roskilde, Denmark, 2001
- [8] L. Johansson, The importance of data availability: Effects of missing or erroneous data, EWEA 2013, Vienna, Austria
- [9] DNVGL (2016), Fatigue design of offshore steel structures, DNVGL-RP-C203.
- [10] M. Hansen, *Aerodynamics of Wind Turbines*, 2nd Ed., Earthscan, London, UK, 2007.
- [11] Siemens brochure, "Thoroughly tested, utterly reliable: Siemens Wind Turbine SWT-3.6-120", Germany, 2011.
- [12] Hasselmann, K., Barnett, T.P. et al., "Measurements of wind-wave growth and swell decay during the Joint North Sea Wave Project (JONSWAP)" TU Delft, 1973.
- [13] Jocelyn Frechet "REALISTIC SIMULATION OF OCEAN SURFACE USING WAVE SPECTRA"
- [14] "Nvidia CUDA C Programming Guide", NVIDIA, 2014